MODELLING THE VAPORIZATION OF CRYOGENIC LIQUID SPILLED ON THE GROUND CONSIDERING DIFFERENT BOILING PHENOMENA

Yi Liu[1], Xiaodan Gao[1], Tomasz Olewski[2], Luc Vechot[2] and M. Sam Mannan[1,*]
[1]Mary Kay O'Connor Process Safety Center, Artie McFerrin Department of Chemical Engineering, Texas A & M University, College Station, TX 77843, USA
[2]Texas A&M University at Qatar, PO Box 23874, Education City, Doha, Qatar
*Corresponding author: mannan@tamu.edu

The formation of a vapor cloud following the spill of cryogenic hazardous liquid on ground presents significant fire or toxic hazards. Predicting the evaporation rate is central for risk assessment purpose to estimate the consequences of the cryogenic liquid spill. Numerical simulation is performed to study the heat transfer from the ground to the liquid pool during the vaporization process. Sensitivity analysis is carried out and a set of optimized simulation parameters with a domain size of 0.2 m, a space resolution of 0.2 mm, and a time resolution of 20 ms is chosen. The effect of different boiling modes on the heat transfer is further studied using a boiling curve to specify the boundary condition. Three different boiling stages – film boiling, transition boiling and nucleate boiling – are identified. The heat flux across the ground surface to the liquid pool is discussed during the whole cooling process following the cryogenic liquid spill on the ground. The ability of this numerical model to consider complex boiling phenomena is encouraging as its further development would potentially provide an accurate description of the source term model of vapor formation during cryogenic liquid spill.

KEYWORDS: Vaporization, cryogenic liquid, heat conduction, boiling, source term model, LNG

1. INTRODUCTION

Natural gas (NG) has become one fast-growing source of energy in the world driven by the needs for cleaner energy, the relative low price of NG, and its abundant supplies. When NG is liquefied, its volume is reduced by about 620 times, thus makes it easier to be transported and stored. Many onshore or offshore LNG import terminals are expected to be constructed in the future several years to meet the significant increase in LNG importation from overseas as a result of growing demand[1,2]. Nowadays the natural gas consumption makes up to 24% of the overall energy consumption in the US, 3% of that is imported in the form of LNG. However, when LNG is spilled on the ground or water, the formed flammable vapor cloud brings significant fire and explosion hazards. And although the history of LNG, which begun in the late forties of the twentieth century, has a quite good record compared to other fossil fuels, fatal accidents happened. The biggest one occurred on 20th of October 1944 in Cleveland, Ohio, where an incorrectly designed tank failed soon after being put into service, causing a LNG release and the formation of flammable vapor cloud. The vapor cloud was ignited and the explosion led to the death of 128 people[3].

LNG is usually stored at atmospheric pressure and at its atmospheric pressure boiling temperature of approximately -162°C. If there is any spill or loss of containment, flammable vapor (predominately methane) will be produced due to the heat transfer to the liquid pool. The initially cold vapor resulting from vaporization will be denser than air and forms a dense cloud close to the ground, which is pushed downwind. If an ignition source of sufficient energy is present where a vapor cloud exists at a 4.4%–17% concentration in air, the vapor cloud can ignite and burn. The ability of predicting the vaporization rate of such event is essential for risk assessment of safe separation distances for flammable vapor dispersion and thermal radiation from pool fire. Numerous researches have been performed on the modeling of the vapor cloud dispersion[4-10]. However LNG dispersion analysis is significantly affected by the estimation of source term. An accurate source term model is necessary to reduce the uncertainty of the subsequent dispersion model.

Generally, the source term model of LNG vapor formation is dominated by the heat transfer from the ground to the liquid pool. The existence of boiling generates bubbles of vapor or a vapor film at the liquid-ground interface depending on the temperature difference between the liquid and the ground. This makes this heat transfer process more complex to predict. Some experimental work has been done to measure the boiling curve (heat flux vs. temperature difference between the liquid and the ground) of cryogenic liquid, such as liquid nitrogen[11,12] and LNG[13]. Liu *et al*[14] developed a CFD methodology to simulate the boiling process at different ground temperatures, and found the simulated boiling curve to be comparable to the experimental data. This approach may be used to calculate the boiling curve for complex cryogenic liquid, e.g. methane, LNG.

In this paper, the heat transfer inside a concrete ground and at the interface between the ground and the liquid pool are simulated numerically using MATLAB software. Liquid nitrogen is used as an analog of LNG for this investigation due to the simple composition (pure liquid), easy cross

comparison with literature data. In addition future validation of the approach will be safer when performed with liquid nitrogen than LNG as a first approach. The ideal heat transfer inside the ground is simulated numerically as a first attempt ignoring the thermal resistance between the liquid pool and the ground during boiling process. A sensitivity analysis is performed on different computational domain sizes (0.1 ∼ 0.4 m), space resolutions (mesh size, 0.2–2 mm), mesh geometry (uniform, incremental) and time resolutions (time step, 2–20 ms). The numerical simulation results are compared to the analytical results in order to define a set of optimized parameters to be used for the numerical method. The numerical model is subsequently improved by considering the thermal resistance resulting from the existence of a layer of generated bubbles on the interface between the ground and liquid pool during the boiling process. The effect of different boiling modes on the total heat flux across the ground surface is discussed.

2. THEORY OF 1D TRANSIENT SEMI-INFINITE HEAT CONDUCTION

A cryogenic liquid spill on an initially hot ground surface will cause this surface temperature to decrease over time. With the assumption of an infinite horizontal pool size, the heat conduction through the ground can be reduced to a one-dimensional (1D) semi-infinite vertical unsteady-state conduction problem described by the Fourier's equation

$$\frac{\partial^2 T}{\partial x^2} = \frac{1}{\alpha}\frac{\partial T}{\partial t} \tag{1}$$

2.1 ANALYTICAL SOLUTION FOR PERFECT THERMAL CONTACT BETWEEN THE LIQUID AND THE GROUND

If perfect thermal contact between the liquid and the ground is assumed, and the ground surface temperature is considered to be constant at the boiling point of the liquid, the solution of equation (1) can be described as[15]:

$$T = T_a - (T_a - T_b)\mathrm{erfc}(x/2\sqrt{\alpha t}), \tag{2}$$

where T_a is the initial ground temperature, T_b the liquid boiling point, x the distance downwards from the ground surface, α is thermal diffusivity of the ground. The heat flux q across the ground surface can be calculated as[15]:

$$q = k\frac{\partial T}{\partial x}\bigg|_{x=0} = \frac{k(T_a - T_b)}{\sqrt{\pi\alpha t}}. \tag{3}$$

2.2 NUMERICAL SOLUTIONS AND BOUNDARY CONDITIONS

If the forward-difference approximation is used for time and central-difference form for space, the finite-difference form of equation (1) is represented by[16]

$$\begin{aligned} T_x^{t+\Delta t} &= T_x^t + \frac{\alpha\Delta t}{(\Delta x)^2}(T_{x+\Delta x}^t - 2T_x^t + T_{x-\Delta x}^t) \\ &= T_x^t + n(T_{x+\Delta x}^t - 2T_x^t + T_{x-\Delta x}^t), \end{aligned} \tag{4}$$

where

$$n = \frac{\alpha\Delta t}{(\Delta x)^2}. \tag{5}$$

When the boundary temperatures are known, the finite difference equation above can be employed to calculate the temperature of the internal grid points as a function of time. Generally, the problem is stable when,

$$n = \frac{\alpha\Delta t}{(\Delta x)^2} < 0.5. \tag{6}$$

For a space resolution (Δx) of 0.2 mm, the time resolution (Δt) should be smaller 29 ms for a heat diffusion coefficient of 7×10^{-7} m^2/s.

When the thermal resistance between the ground surface and the liquid pool is ignored, corresponding to *perfect thermal contact between the liquid and the ground*, then a Dirichlet type of boundary condition can be adopted, e.g., the fluid temperature adjacent to the ground surface equals to the liquid boiling point (T_b = 77 K for liquid nitrogen), then

$$T_0^{t+\Delta T} = T_0^t + n(T_{\Delta x}^t - 2T_0^t + T_b) \tag{7}$$

$$q^{t+\Delta t} = \frac{k}{\Delta x}(T_{\Delta x}^t - T_0^t) \tag{8}$$

Dirichlet boundary condition is suitable for liquid pool without boiling. However, it is not valid when boiling occurs. In this case, the thermal resistance between the ground surface and the liquid pool should not be ignored anymore. A Neumann type of boundary condition can be adopted if the heat flux q between the ground surface and the liquid pool is already known, and the ground surface temperature can be calculated by

$$T_0^{t+\Delta T} = T_0^t + n\left(T_{\Delta x}^t - T_0^t + \frac{\Delta x}{k}q^t\right). \tag{9}$$

3. VERIFICATION AND OPTIMIZATION OF SIMULATION PARAMETERS

To verify the numerical simulation and to optimize a set of simulation parameters, the ideal 1D transient semi-infinite conduction problem is studied by numerical simulation of a finite conduction using MATLAB software. Figure 1 shows the procedure of numerical simulation. Concrete is considered as the ground material, and some constant physical properties are specified as averaged values based on literature data[17–20] as below, ρ = 2300 kg/m^3, k = 1.61 W/m · K, c_p = 1000 J/kg · K, $\alpha = 7 \times 10^{-7}$ m^2/s.

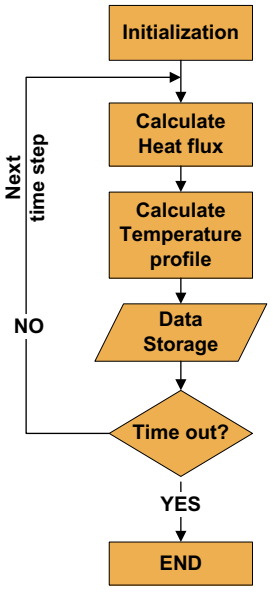

Figure 1. Flow sheet of numerical simulation

The analytical solutions of equations (2) and (3) are employed to verify the simulation results.

Different simulation parameters such as computational domain sizes, time resolutions, space resolutions and mesh geometries are studied. The effects of them on the accuracy of the simulation results are compared, and ultimately a set of optimized simulation parameters is identified.

To simulate the 1D semi-infinite conduction process on an infinite computation domain, it is of major importance to determine a suitable computation domain size (D_c). A concept of critical depth (x_c) is proposed. It is defined as the distance from the ground surface to a point, where the ground temperature T meets the below criterion,

$$\frac{T - T_b}{T_a - T_b} = 0.99. \tag{10}$$

The time to reach this state is defined as critical time (t_c). According to equation (2), the critical depth can be calculated as a function of critical time,

$$x_c \approx 3.643\sqrt{\alpha t_c}. \tag{11}$$

The effect of the domain size can be ignored only if the computational domain size is larger than the critical depth,

$$D_c \geq x_c. \tag{12}$$

Generally, for concrete with a heat diffusion coefficient of 7×10^{-7} m^2/s, a typical critical depth will be 0.2 m at a critical time of 1 h, which means the computational domain size should be larger than 0.2 m.

Figure 2 shows the temperature profiles in the concrete at 1 hour and heat flux evolutions simulated at different computational domains (0.40, 0.20, 0.13 and 0.10 m), space resolutions (0.2, 0.5, 1 and 2 mm), time resolutions (2, 5, 10 and 20 ms), and mesh geometries (uniform or incremental meshes). The differences between numerical and analytical heat fluxes at the ground surface are summarized in Table 1.

Figure 2a and 2b show the effect of different computational domain sizes. For the domains of 0.40 m and 0.20 m, the temperature profiles resulting from the numerical simulation are similar to that from the analytical solution (equation (2)). The heat fluxes are very close to the analytical result for a period of 1 hour with a maximum difference of -0.11% only at the initial several seconds. For the domains of 0.13 m and 0.10 m, the difference between numerical and analytical heat fluxes is noticeable after 30 minutes, and it ultimately reaches $+0.25\%$ and $+3.78\%$ at 1 hour respectively. It shows that a domain larger than 0.20 m is large enough for current study. However, a domain of 0.13 m is also acceptable if only the heat flux at the ground surface is concerned rather than the temperature profile.

Figure 2c and 2d show the effect of different space resolutions. It is found the space resolution play a more important role in the early stage (during 0$\sim$60s) of the simulation. The difference between numerical and analytical heat fluxes can be as large as -36.7% or -10.5% at the first second for a sparse space resolution of 2 or 1 mm. However, it quickly turns smaller than -1% after 36 or 9 seconds. For a medium space resolution of 0.5 mm, the difference between numerical and analytical heat fluxes can be -2.05% at the first second. For a dense space resolution of 0.2 mm, the difference is only -0.11%. The rapid reduction of the difference between simulated and analytical heat fluxes at a denser space resolution can be well explained by the truncation error during the numerical simulation. When a first-order derivative is approached by finite difference method, the discretization error can be of an order Δx for forward-difference or backward-difference whereas it is of an order $(\Delta x)^2$ for central-difference or second-order derivative[16]. So the difference can be reduced from -36.7% to be -0.11%, which is of the order 100, when the space resolution is decreased by 10 times from 2 to 0.2 mm. Generally, a dense space resolution of 0.2 mm will provide more accurate results however at the expense of simulation time.

The effect of mesh geometry is also studied. To reduce the simulation time, sometimes it is necessary to use a non-uniform mesh instead of uniform mesh. Several incremental meshes with different fixed incremental factors (IF), defined as the ratio of the sizes of two adjacent meshes, are compared to the uniform mesh (IF = 1) and the analytical results. Although the temperature profiles show much different from the analytical result for a large IF, it is found the heat fluxes at the ground surface change little with the IF (Figure 2e and 2f). The maximum difference between the simulated and the analytical heat fluxes is 0.43% with an IF equal to 1.20. However, the mesh number reduces from 1000 to 29, which saves about 97% of the simulation time.

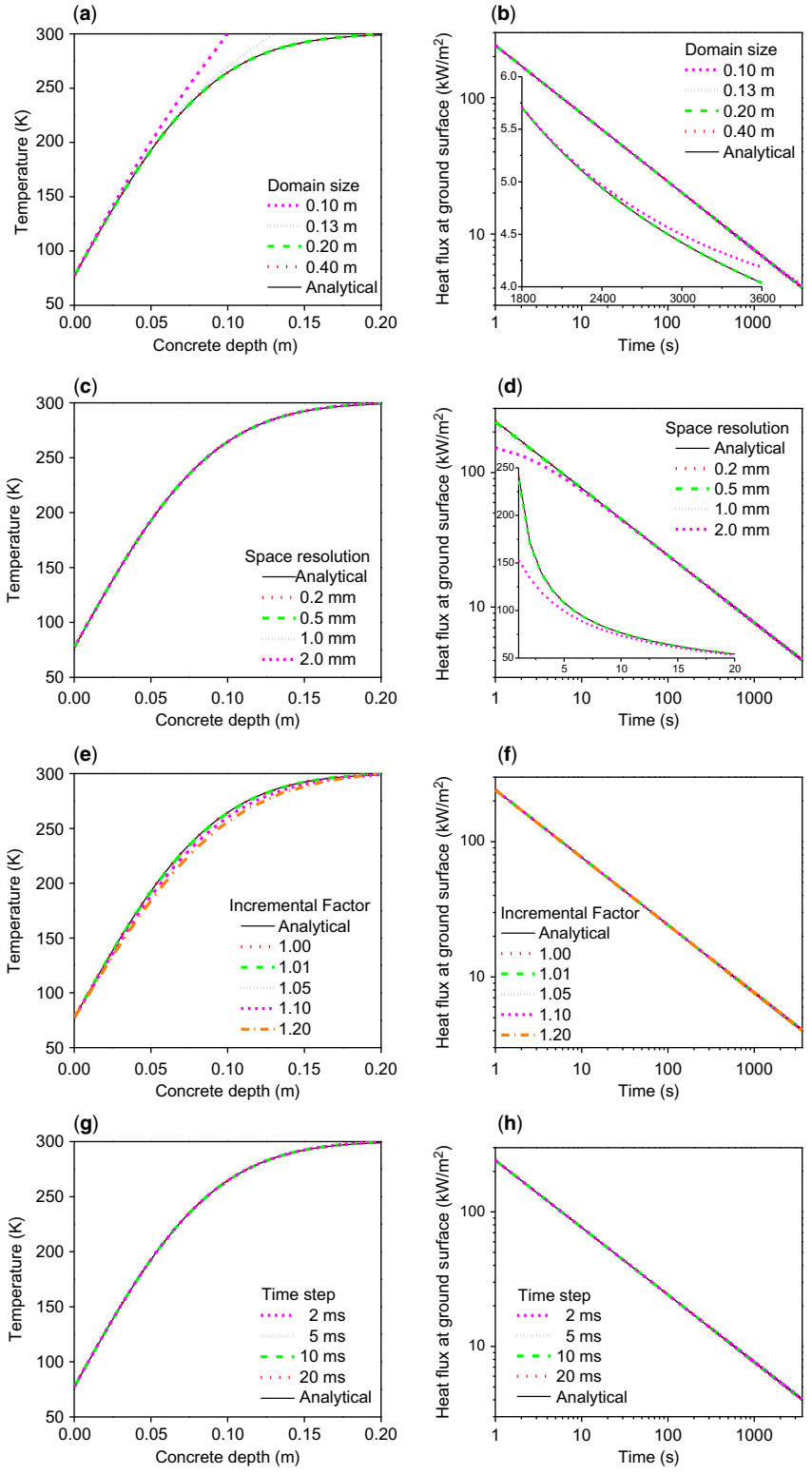

Figure 2. Temperature profiles at 1 hour (a, c, e, g) and evolutions of the heat flux at ground surface (b, d, f, h) simulated at different domain sizes (a, b), space resolutions (c, d), mesh geometries (e, f) and time resolutions (g, h)

Table 1. Summary of differences between simulation and analytical heat flux at the ground surface at different simulation parameters*

Domain size (m)		Space resolution (mm)		Mesh IF		Time resolution (ms)	
	Difference (%)		Difference (%)		Difference (%)		Difference (%)
0.40	−0.11	0.2	−0.11	1.00	−0.11	30	Divergent
0.20	−0.11	0.5	−2.05	1.01	−0.11	20	−0.11
0.13	+0.25	1	−10.5	1.02	−0.12	10	−0.23
0.10	+3.78	2	−36.7	1.05	−0.15	5	−0.30
				1.10	−0.22	2	−0.33
				1.20	−0.43		

* For sensitivity study of each parameter, the other parameters are default: domain size – 0.2 m; space resolution – 0.2 mm; mesh IF – 1.00; time resolution – 20 ms.

Figure 2g and h show the effect of different time resolutions. The temperature profiles and the heat fluxes at the ground surface resulting from the numerical simulation are similar to those from the analytical solutions (equation (2) and (3)) for different time resolutions from 2 ms to 20 ms. The differences between numerical and analytical heat fluxes are smaller than 0.33%. However, if the time resolution is larger than 29 ms, the solution will be divergent, which is consistent with the stability criterion of equation (6). To decrease the simulation time, the time resolution should be as large as possible. So a time resolution of 20 ms is suitable for current study.

4. HEAT TRANSFER FROM GROUND DURING BOILING PROCESS

The boiling process during a cryogenic liquid spill on the ground will obviously affect the cooling process of the ground. Compared to the analytical solution of the ideal conduction case, where the ground surface temperature is assumed equal to the liquid pool temperature (77 K in case of liquid nitrogen spill), the ground surface temperature during a boiling process is higher than the liquid pool temperature. During the boiling process, some isolated bubbles and/or a continuous vapor film will be generated between the ground surface and the liquid pool[14]. These bubbles or vapor film reduce the heat transfer allowing the ground surface temperature to be much higher than the liquid temperature. A sketch is shown in Figure 3. The temperature difference between the ground surface and the liquid pool may be as large as 200 K at the early stage of spill and it decreases with time. It will affect the boiling phenomenon and ultimately the heat flux rate to the pool, which is different for each of the boiling regime[14]. Thus, it seems to be very important to include boiling regimes into the source term model.

During the boiling process, the heat flux q from the ground to the liquid pool is determined by the temperature difference between the liquid pool boiling point (T_b) and the ground surface temperature (T_0^t). Figure 4 shows an experimental boiling curve of liquid nitrogen[11]. Generally, at a low value of the temperature difference, the heat flux increases with the temperature difference; at a medium value, the temperature difference represents a negative effect on the heat flux; while at a high value of the temperature difference, the heat flux increases with it again. These three different processes are identified as nucleate boiling, transition boiling and film boiling respectively[11,12].

At the early stage of cryogenic liquid spill, the temperature difference between the liquid pool and the ground surface is very large, and the boiling at this stage belongs to film boiling. With the boiling progresses, the ground temperature decreases, and the heat flux at the ground surface

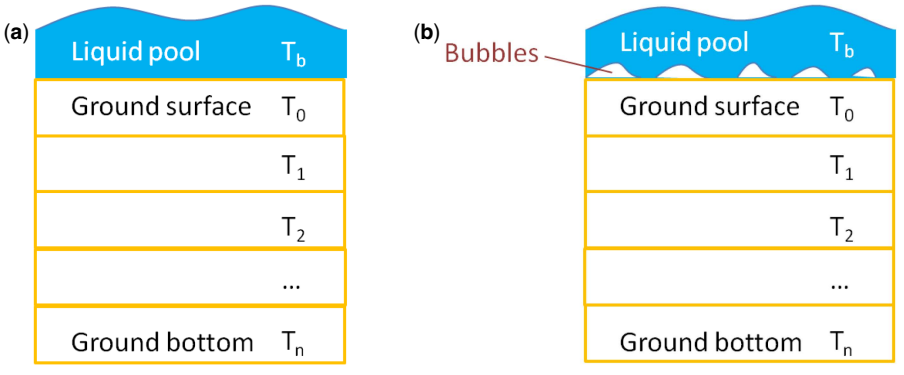

Figure 3. Boundary conditions at the ground surface: (a) No boiling ($T_0 = T_b$); (b) Boiling ($T_0 > T_b$)

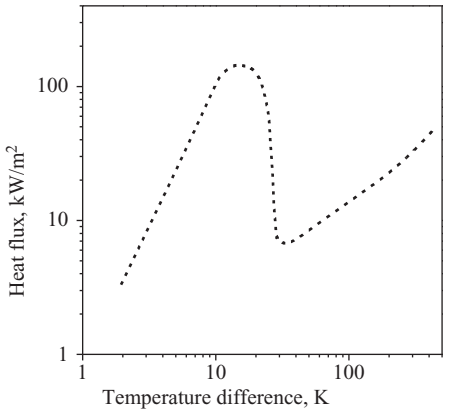

Figure 4. Boiling curve of liquid nitrogen[11]

also reduces, because temperature difference between the liquid pool and the ground surface also decreases. At a critical ground temperature (referred as Leidenfrost point[14]), the boiling will turns into transition boiling. In the transition stage, the ground temperature continues to decrease; however, the heat flux at the ground surface begins to increase. The increased heat flux makes the surface temperature reduce more quickly. The transition boiling is accelerated and it only lasts for a short period before the boiling turns into the nucleate boiling. During the nucleate boiling stage, the ground temperature gradually approach to the liquid boiling point, and the heat flux continues to decrease with the ground temperature. The nucleate boiling will last for a long period due to the low heat flux with a small temperature difference.

In this paper, the above described model of the ground's "non-ideal" cooling process is studied by the MATLAB (version 7.10.0) code with the parameters developed in a Section 3. The developed model is an attempt to improve analytical solution of the "ideal" conduction and incorporates different boiling regimes, which governs the heat flux rate to the cryogenic liquid pool. A Neumann type of boundary condition is adopted**.** The experimental boiling curve is applied to correlate the heat flux with the temperature difference between the ground surface and the liquid pool, which will be substituted into equation (8) to perform the numerical simulation.

The comparison of numerical solution of the ideal conduction with developed model, which include boiling regimes, is shown in Figure 5. The result from the analytical solution leads to the heat flux at the beginning of the spill is equal to infinity and during first seconds can be as large as 240 $kW \cdot m^{-2}$. At the same time, the surface temperature is immediately equal to the liquid's boiling point (77 K for liquid nitrogen). These are represented by dashed lines in Figure 5. In contrast to these, the ground temperature at the early stage of spill, when the boiling process is considered, is far higher than the liquid's boiling point (solid line in Figure 5a) whereas the heat flux is much reduced by vapor film. The reduced heat flux at the initial film boiling stage may be as small as 24 $kW \cdot m^{-2}$, which is only one tenth of that of ideal conduction, and, according to our estimations, this regime can lasts about 25 min (solid line in Figure 5b).

Following the film boiling regime, the rapid rise of the heat flux is observed due to the transition from film boiling to nucleate boiling regime, while the ground surface temperature decreases suddenly (at time about 1500 s). The transition boiling stage only lasts about 30 seconds before the heat flux reach a maximum value. Then the nucleate boiling stage begins. The heat flux decrease quickly and the ground surface temperature continues to decrease and approach the liquid boiling point (77 K). The result of nucleate boiling regimes shows it is similar to the ideal solution and is almost the same at very late stage. However it must be note that at this stage the ground temperature is already very low and the spill has to last for a long time.

Figure 6 shows the ground temperature profiles at different boiling regimes. The ground temperature profile up to the depth of about 7 cm is much different from the ideal solution at the duration of 0.25 hr, which represents the film boiling regime. Whereas, is almost the same for the nucleate boiling regime (shown in Figure 6 at 1 hr), when the modeled temperature profile approaches the ideal conduction case.

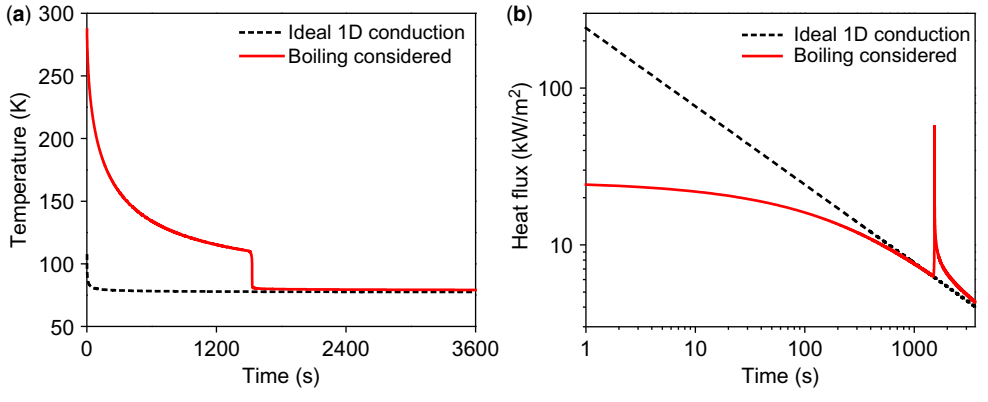

Figure 5. Evolutions of (a) surface temperature and (b) surface heat flux when boiling process is considered at different mesh geometries

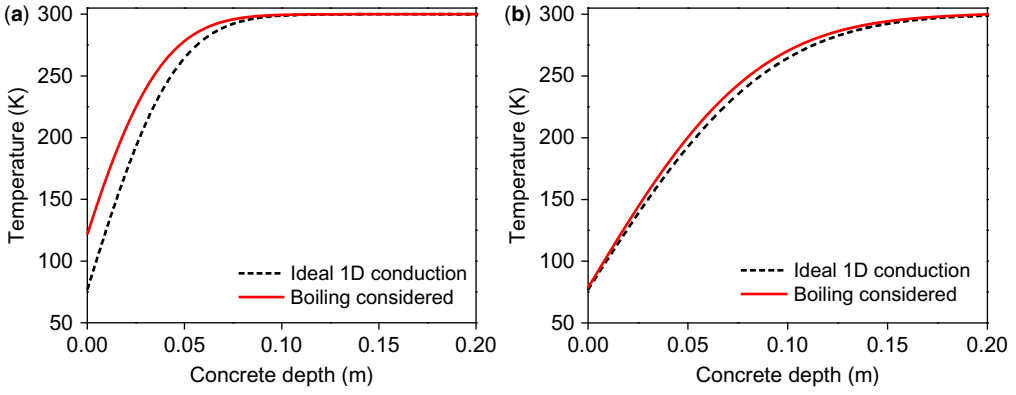

Figure 6. Ground temperature profiles for: (a) film boiling (at 0.25 hr of spill duration); and (b) nucleate boiling (at 1 hr)

5. CONCLUSIONS

The semi-infinite conduction problem following the cryogenic liquid spill on the ground is studied by numerical simulation in MATLAB. The validation of the numerical solution of the "ideal" conduction model as well as parameters' sensitivity and optimization has been performed. Validation has proved that the numerical solution can be used with the recommendation of the optimized parameters. Parameters' sensitivity analysis was performed on computational domain size, space resolution, mesh geometry, and time resolution. A set of following simulation parameters is recommended for the numerical solving of the conduction problem of the ground below the cryogenic liquid: the domain size (ground depth) of 0.2 m, the space resolution of 0.2 mm, and the time resolution of 20 ms. An incremental mesh with a IF up to 1.20 can greatly decrease the simulation time with few reduction of accuracy. The ability of this numerical model to consider complex boiling phenomena is encouraging as its further development would provide more accurate description of the source term model of vapor formation during cryogenic liquid spill.

The heat conduction process from the ground to the liquid pool, considering the thermal resistance of vapor film during the boiling process, was performed utilizing the experimental boiling curve from literature to specify the boundary condition. Three different boiling stages – film, transition and nucleate boiling – are identified during the whole ground cooling process following cryogenic liquid spill on ground. The heat flux and ground surface temperature evolution of presented model show big difference from ideal solution, which will result in lower vaporization rate at the early stage of the cryogenic liquid spill and much longer its duration. Future validation of the model with experimental data for liquid nitrogen, methane or LNG is needed and will be performed.

ACKNOWLEDGEMENT

The authors would like to thank BP Global Gas SPU for their financial support and guidance. They also acknowledge the support of Qatar Petroleum in the form of the facilities used for experiments at Ras Laffan Industrial City and the provision of staff to work with the Texas A&M University at Qatar's LNG research team.

NOMENCLATURE

C_p	Specific heat capacity at constant pressure ($kJ \cdot kg^{-1} \cdot K^{-1}$)
D_c	Computational domain size (m)
m	A dimensionless parameter defined as $\frac{T - T_b}{T_a - T_b}$
n	A dimensionless parameter defined as $\frac{\alpha \Delta t}{(\Delta x)^2}$
k	Thermal conductivity of ground ($W \cdot m^{-1} \cdot K^{-1}$)
q	Heat flux at the ground surface ($W \cdot m^{-2}$)
q^t	Heat flux at the ground surface at a time of t ($W \cdot m^{-2}$). Similar as $q^{t+\Delta t}$
T	Temperature (K)
T_a	Initial ground temperature (K)
T_b	Liquid boiling point (K)
T_x^T	Ground temperature at a distance of x from the ground surface and a time of t (K) Similar as $T_{\Delta x}^t$, $T_{x+\Delta x}^t$, $T_{x-\Delta x}^t$, $T_{x+2\Delta x}^t$, $T_{x-2\Delta x}^t$, $T_x^{t+\Delta t}$, $T_{x+\Delta x}^{t+\Delta t}$, $T_{x-\Delta x}^{t+\Delta t}$.
T_0^t	Ground temperature at the surface and a time of t (K) Similar as $T_0^{T+\Delta t}$
t	Time (s)
t_c	Critical time (s)
x	Distance downwards from the ground surface (m)
x_c	Critical depth (m)
α	Thermal diffusivity of ground ($m^2 \cdot s^{-1}$)
ρ	Density of ground ($kg \cdot m^{-3}$)
Δt	Time resolution (s)
Δx	Space resolution (m)

REFERENCES

1. Hightower, M., M. Gritzo, L. A., Luketa-Hanlin, A. J., Covan, J. M., Tieszen, S., Wellman, G. W., Irwin, M. J., Kaneshige, M. J., Melof, B. M., Morrow, C. W.,

Ragland, D., "Guidance on risk analysis and safety implications of a large liquefied natural gas (LNG) spill over water," Sandia National Laboratories, 2004.
2. Thorndike, V. L. *LNG: A Level-Headed Look at the Liquefied Natural Gas Controversy*; Down East Books 2007.
3. "Report on the Investigation of the Fire at the Liquefaction, Storage, and Regasification Plant of East Ohio Gas Co., Cleveland, Ohio, October 20, 1944," U.S. Bureau of Mines, 1946.
4. Cormier, B. R., Qi, R., Yun, G., Zhang, Y., Sam Mannan, M., Application of computational fluid dynamics for LNG vapor dispersion modeling: A study of key parameters, *Journal of Loss Prevention in the Process Industries*, *22*, 332–352, 2009.
5. Yun, G., Ng, D., Mannan, M. S., Key Observations of Liquefied Natural Gas Vapor Dispersion Field Test with Expansion Foam Application, *Industrial & Engineering Chemistry Research*, *50*, 1504–1514, 2011.
6. Rana, M. A., Guo, Y., Mannan, M. S., Use of water spray curtain to disperse LNG vapor clouds, *Journal of Loss Prevention in the Process Industries*, *23*, 77–88, 2010.
7. Gavelli, F., Bullister, E., Kytomaa, H., Application of CFD (Fluent) to LNG spills into geometrically complex environments, *Journal of Hazardous Materials*, *159*, 158–168, 2008.
8. Hansen, O. R., Gavelli, F., Ichard, M., Davis, S. G., Validation of FLACS against experimental data sets from the model evaluation database for LNG vapor dispersion, *Journal of Loss Prevention in the Process Industries*, *23*, 857–877, 2010.
9. Olewski, T., Nayak, S., Basha, O., Waldram, S., Véchot, L., Medium scale LNG-related experiments and CFD simulation of water curtain, *Journal of Loss Prevention in the Process Industries*, *24*, 798–804, 2011.
10. Basha, O., Olewski, T., Waldram, S., In *13th Annual Symposium, Mary Kay O'Connor Process Safety Center*; Texas A&M University, College Station, Texas: College Station Hilton Conference Center, College Station, Texas, 2010; Vol. 1; pp. 935–945.
11. Berenson, P. J., Experiments on pool-boiling heat transfer, *International Journal of Heat and Mass Transfer*, *5*, 985–999, 1962.
12. Barron, R. F., *Cryogenic heat transfer*; Taylor and Francis: Philadelphia, PA, US, 1999.
13. Wursig, G. M., Gaughan, J., Scholz, B., Sannes, L., Kabelac, S., Leder, A., Effect of enveloping pool fires on LNG tank containment systems. *GasTech Conference*: AbuDhabi, UAE, May 2009.
14. Liu, Y., Olewski, T., Véchot, L., Mannan, M. S., In *Mary Kay O'Connor Process Safety Center International Symposium*: College Station, TX, US, 2011.
15. Briscoe, F., Shaw, P., Spread and Evaporation of Liquid, *Progress in Energy and Combustion Science*, *6*, 127–140, 1980.
16. Wong, K.-F. V., *Intermediate heat transfer*; Marcel Dekker, Inc.: New York, 2003.
17. Dahmani, L. Thermomechanical response of LNG concrete tank to cryogenic temperatures. *Strength of Matrials, 43,* 526–531, 2011.
18. Tandiroglu, A. Temperature-dependent thermal conductivity of high strength lightweight raw perlite aggregate concrete. *Int J Thermophys, 31*, 1195–1211, 2010.
19. Kim, K.H., Jeon, S.E., Kim, J.K., Yang, S. An experimental study on thermal conductivity of concrete. *Cement and concrete research, 33*, 363–371, 2003.
20. Guo, L., Guo, L., Zhong, L., Zhu, Y., Thermal conductivity and heat transfer coefficient of concrete. *Journal of Wuhan University of Technology-Mater. Sci. Ed., 26*, 791–796, 2011.